Published in final edited form as:
Horbens, M., Eder, M., & Neinhuis, C. (2015). A materials perspective of Martyniaceae fruits: Exploring structural and micromechanical properties. *Acta Biomaterialia, 28*, 13-22. doi:10.1016/j.actbio.2015.10.002.

A materials perspective of Martyniaceae fruits: Exploring structural and micromechanical properties

Abstract

Several species of the plant family Martyniaceae are characterised by unique lignified capsules with hook-shaped extensions that interlock with hooves and ankles of large mammals to disperse the seeds. The arrangement of fruit endocarp fibre tissues is exceptional and intriguing among plants. Structure–function-relationships of these slender, curved, but mechanically highly stressed fruit extensions are of particular interest that may inspire advanced biomimetic composite materials. In the present study, we analyse mechanical properties and fracture behaviour of the hook-shaped fruit extensions under different load conditions. The results are correlated with calculated stress distributions, the specific cell wall structure, and chemical composition, providing a detailed interpretation of the complex fruit tissue microstructure. At the cell wall level, both a large microfibril angle and greater strain rates resulted in Young's moduli of 4–9 GPa, leading to structural plasticity. Longitudinally arranged fibre bundles contribute to a great tensile strength. At the tissue level, transversely oriented fibres absorb radial stresses upon bending, whereas cells encompass and pervade longitudinal fibre bundles, thus, stabilise them against buckling. During bending and torsion, microcracks between axial fibre bundles are probably spanned analogous to a circular anchor. Our study fathoms a highly specialized plant structure, substantiating former assumptions about epizoochory as dispersal mode. While the increased flexibility allows for proper attachment of fruits during dynamical locomotion, the high strength and stability prevent a premature failure due to heavy loads exerted by the animal.

Full Length Article

A materials perspective of Martyniaceae fruits: exploring structural and micromechanical properties

Melanie Horbens[a,*], Michaela Eder[b], and Christoph Neinhuis[a]

[a]Institute for Botany, Technische Universität Dresden, Zellescher Weg 20b, 01062 Dresden, Germany

[b]Department of Biomaterials, Max-Planck-Institute of Colloids and Interfaces, Am Mühlenberg 1 OT Golm, 14476 Potsdam, Germany

Email addresses and phone/fax numbers:

*author for correspondence: Melanie Horbens, melanie.horbens@tu-dresden.de, tel. ++49 351 463 31497, fax ++49 351 463 37032

Michaela Eder, michaela.eder@mpikg.mpg.de, tel. ++49 331 5679422, fax ++49 331 5679402

Christoph Neinhuis, christoph.neinhuis@tu-dresden.de, tel. ++49 351 463 36032, fax ++49 351 463 37032

Abstract

Several species of the plant family Martyniaceae are characterised by unique lignified capsules with hook-shaped extensions that interlock with hooves and ankles of large mammals to disperse the seeds. The arrangement of fruit endocarp fibre tissues is exceptional and intriguing among plants. Structure-function-relationships of these slender, curved, but mechanically highly stressed fruit extensions are of particular interest that may inspire advanced biomimetic composite materials. In the present study, we analyse mechanical properties and fracture behaviour of the hook-shaped fruit extensions under different load conditions. The results are correlated with calculated stress distributions, the specific cell wall structure, and chemical composition, providing a detailed interpretation of the complex fruit tissue microstructure. At the cell wall level, both a large microfibril angle and greater strain rates resulted in Young's moduli of 4–9 GPa, leading to structural plasticity. Longitudinally arranged fibre bundles contribute to a great tensile strength. At the tissue level, transversely oriented fibres absorb radial stresses upon bending, whereas cells encompass and pervade longitudinal fibre bundles, thus, stabilise them against buckling. During bending and torsion, microcracks between axial fibre bundles are probably spanned analogous to a circular anchor. Our study fathoms a highly specialized plant structure, substantiating former assumptions about epizoochory as dispersal mode. While the increased flexibility allows for proper attachment of fruits during dynamical locomotion, the high strength and stability prevent a premature failure due to heavy loads exerted by the animal.

Keywords:

Fruit endocarp

Fruit hooks

Functional anatomy

Plant biomechanics

Structural hierarchy

1. Introduction

Plants rely on diverse permanent and reversible attachment systems. Besides adhesive roots and pads in climbing plants, hook-shaped epidermal outgrowths enable the interlocking with adjacent supporting plants [1-3]. Furthermore, hooks and barbs are important attachment devices of fruits adapted to epizoochorous dispersal, such as the passive transport upon the body surface of animals [4-6]. Capsules of the plant family Martyniaceae, so-called trample burrs, pursue a very cunning strategy of fruit dispersal. Their hook-shaped fruit extensions interlock with hooves and ankles of large mammals stepping onto the fruits laying on the ground.

With regard to the very slender, curved, but mechanically highly stressed fruit extensions of some Martyniaceae, relationships between structurally optimised plant structures and the resulting mechanical properties are of particular interest that may inspire novel biomimetic materials, especially concerning the arrangement of load-bearing components in composite materials. From a mechanical perspective, transverse stresses especially in curved beams can lead to failure under bending. Curved branches of trees, for example, are known to split along the centric neutral axis if branches are bent to decrease the curvature [7,8]. Plants exhibit a strong hierarchically structured organisation, which means that structure and composition can be adjusted on different length scales, also known from bone or tendon [9,10]. Plant cell walls as polymeric fibre composites are helically reinforced by cellulose microfibrils embedded in into a matrix of lignin, hemicellulose, pectin, and/or glycoproteins. The thickness and compositional modifications combined with the angle of microfibril orientation (MFA) determine stiffness and strength of plant cell walls [10,11]. At the macroscopic level, aggregates of plant cells build a mostly anisotropic cellular solid. The structural organisation and arrangement of different cell types, especially of fibres or tracheids, and the formed tissues largely affect plant mechanics, examined at tree wood or plant stems [9-11]. However, little is known about the anatomy and biomechanics of fruit hooks. Previous studies demonstrated that morphological characteristics influence the contact separation force (1) of single hooks of fruit burrs [12,13], (2) of hooked trichomes on the leaf surface [3], and (3) the breaking load of hooks/grapnels along cirrate leaves or flagella of some climbing palms [1].

In this study, fruits of two representative species have been investigated: (1) *Ibicella lutea* (Lindl.) Van Eselt., native to South America (Brazil) and (2) *Proboscidea louisianica* (Mill.) Thell. subsp. *fragrans* (Lindl.), natively occurring in arid, desert areas of North America (Texas to the Central Mexican plateau). Both annual herbs develop capsules composed of a thick and soft outer layer (exo- and mesocarp), which is shed after desiccation exposing a

woody endocarp upon ripening, characterised by about 8-11 cm long, upwardly curved extensions (Fig. 1A,A1) [14,15]. At fruit maturity, the extension tip splits longitudinally into two parts resulting in a shape, which led to the origin of the common plant names: desert unicorn plants or devil's claws (Fig. 1B). It is assumed that the tapered extensions preferentially interlock with hooves and ankles of even-toed ungulates, which act as vectors [14]. However, reliable data on dispersal are scarce. Our previous, anatomical study revealed a complex arrangement of fibrous tissues within the endocarp having a specific ontogeny, which is exceptional and intriguing among plants [15]. The fruit extensions are reinforced by axially running fibres, densely packed in individual bundles (hereinafter called longitudinal sclerenchyma), entwined and separated by transversely elongated fibres (hereinafter called transverse sclerenchyma) (Fig. 1C,D). Since muscle bundles are enclosed by the loose connective tissue [16], a certain similarity between fruit tissues and the anatomy of a human skeletal muscle tissue may be drawn. Within the capsule wall, the fibre bundles are embedded in a denser mesh of transverse sclerenchyma, circularly encompassing the loculus that contains the seeds (Fig. 1E). This peculiar fibre arrangement has been interpreted as an anatomical adaptation of the fruits to secure the proper attachment and withstand multiple mechanical loads during the transport by animals [15].

In the present study, we pursue a biomechanical approach to determine general mechanical properties of fruit extensions providing a detailed interpretation of their complex microstructure. Mechanical tests (tensile loading, bending, and torsional load conditions) are combined with theoretical considerations of qualitative stress distributions in curved beams and the structural characterisation of fracture surfaces using scanning electron microscopy (SEM). Additionally, comparative tests with samples of scots pine (*Pinus sylvestris* L.) having comparable dimensions are performed. Since the pine trunk tissue is composed of longitudinally oriented, tapered, lignified tracheids, and radially reinforcing wood rays without 'wrapping-round' cells, characteristics of fruit hooks and pine wood can be directly compared, considering previously published data on wood mechanics. We correlate the results with cell wall composition analysed by wet-chemistry and Fourier transformed infrared spectroscopy (FTIR), together with the cell wall microstructure regarding the microfibril orientation, obtained by scanning wide-angle x-ray diffraction (WAXD). The study adds to the limited knowledge of fruit hooks as effective, functionally adapted structures, and provides valuable suggestions for the design of bio-inspired fibre-based composite materials.

2. Materials and methods

2.1. Plant material

Mature fruits from plants of *P. louisianica* subsp. *fragrans* (further *P. louisianica*) and *I. lutea*, grown in the Botanical Garden of the Technical University of Dresden, Germany were collected about 50 days after pollination (see [15] for details). Wood of scots pine (*P. sylvestris*) was purchased from commerce.

2.2. Mechanical testing

Mechanical properties of 25 extensions of different fruits were determined under three load conditions (tension, bending, and torsion), using a Zwick/Roell BZ 2.5/TS1S universal testing machine (Zwick/Roell, Ulm, Germany). Dimensions of samples were measured and averaged at five different locations with an IP67 digital micrometer. At least 20 samples of pinewood with upright annual rings, similar rectangular dimensions and moments of resistance were tested under the same conditions as fruit samples.

2.2.1. Tensile tests combined with DIC

Samples were prepared applying a fine stochastic speckle pattern with white and black paint spray, to provide suitable structures for strain measurements by Digital Image Correlation (DIC). Only the central segments of each fruit extension, 25 mm long, were tested to minimise the effect of curvature. The specimens were clamped by screw grips, pre-loaded with 1.0 N (load cell of max. 1 kN), and stretched at a velocity of 1 mm s^{-1}. Each sample was subjected to a maximal strain of 0.5 % in a first, up to failure in a second test. Force and displacement were recorded during the experiments at a rate of 5 Hz, using a DIC Q-400 system (Dantec Dynamics GmbH, Ulm, Germany) equipped with two 5 MP CCD-cameras and a high intensity LED illumination system (HILIS). Based on the dataset of displacements of individual points on the complete sample surface, axial and transversal strains were determined by the correlation algorithm system Istra4D (Dantec Dynamics GmbH, Ulm, Germany). The facet size of 23 pixels and grid spacing of 17 pixels were chosen [17]. By applying Hooke's law assuming conditions of linear elastic behaviour, the Young's modulus E_t of each tensile test and the maximum tensile strength $\sigma_{t\,max}$ at failure were calculated by

$$E_t = \frac{dF}{d\varepsilon A} \text{ and } \sigma_{t\,max} = \frac{F_{max}}{A}, \quad (1)$$

where F is the applied axial force, A the average cross-sectional area, and ε the calculated mean strain.

2.2.2. Three-point-bending tests

Each fruit extension was firstly bent to a displacement of about 1.5 mm staying within the elastic range, subsequently bent to failure at a velocity of 5 mm s^{-1}. The distance of 40 mm between the supports (designed for small samples) ensured a span-to-diameter ratio of at least 15 minimising the influence of shear [18]. Assuming a straight, pure bending problem caused by a bending moment M_b, the Young's modulus E_b and the maximum bending strength $\sigma_{b\,max}$ at the outer fibre layer of the profile were calculated according to

$$E_b = \frac{L^3}{48I}\frac{dF}{dw} \text{ and } \sigma_{b\,max} = \frac{M_{b\,max}}{I}\frac{a}{2}, \quad (2)$$

where L is the distance between the supports, F the applied force, w the corresponding deflection of the sample, and I the average second moment of inertia (for elliptical cross sections of fruit extensions defined by $ba^3\pi/16$, for rectangular cross sections of pinewood by $ba^3/12$ with the height a and width b) [19].

2.2.3. Torsion tests

In torsion tests, the free end of each sample was initially twisted by an angle of 5°, subsequently, twisted up to sample failure or a significant decrease of force using a calibrated additional device module (including a V-belt pulley) at the universal testing machine. The shear modulus G (determined from torsion tests) and the maximum torsional strength τ_{max} were calculated according to

$$G = \frac{dFr}{d\varphi}\frac{l}{J} \text{ and } \tau_{max} = \frac{M_{t\,max}}{W_t}. \quad (3)$$

Here M_t is the applied torque, which was transferred by the force F of the universal testing machine and the radius r of a V-belt pulley, l the sample length (central segments 30 mm long), φ the twist angle in radians (defined by the ratio of the arc length x (traverse distance) to the radius r), and J the average polar second moment of area of samples (for elliptical cross sections of fruit extensions defined by $\frac{\pi}{16}\frac{a^3b^3}{a^2+b^2}$ (a/b≥1), for rectangular cross sections of pinewood by $0.141ab^3$ (1≤a/b≤1.5) with the height a and width b). W_t describes the geometrical resistance against torque, defined by $ab^2\pi/16$ (a/b≥1) for elliptical cross sections, by $0.208ab^2$ (1≤a/b≤1.5) for rectangular cross sections [19].

2.3. Wet-chemical analysis

The acid-insoluble lignin (*Klason* lignin) of fruits was isolated and gravimetrically quantified based on the hydrolysis of cellulose and hemicelluloses using the TAPPI standard procedure T 222 om-11. Furthermore, the cellulose content was determined quantitatively according to the method of Kürschner and Hoffer [20] based on the oxidation and nitration of lignin and the hydrolysis of hemicelluloses leaching these components by Nitric acidic alcohol. Samples

(1 g) including 25 ml Nitric acid (65 %) were boiled three times under reflux for 1 h, washed with ethyl alcohol and water, boiled again with 100 ml water under reflux, filtrated, dried, and weighed.

2.4. Fourier transformed infrared spectroscopy (FTIR)

To analyse specific cell wall components in fruit extensions and Scots pine, one milled sample of each species was investigated using a FT-spectrophotometer Vector 33 (Bruker Biospin Corporation, Billerica, MA, USA). FTIR spectra were recorded by direct transmittance from 4000 to 400 cm^{-1}, with 60 cumulative scans at a spectral resolution of 2 cm^{-1}. Post-spectroscopic manipulations (peak-normalisation, baseline-correction) have been omitted, since an equal total amount of individual cell wall components (e.g. lignin) of the different species was not expected.

2.5. Wide-angle x-ray diffraction (WAXD)

The mean orientation of the cellulose microfibrils across the cell walls of the fruit endocarp (44 day old fruits) was measured by wide-angle x-ray diffraction (WAXD) using synchrotron radiation with a wavelength λ of 0.8266 Å and energy of 15 keV at the µ-Spot beamline at BESSY II (Berlin, Germany). Longitudinal and transversal, ~ 40 µm thick and 480 – 2650 µm wide slices were dried and afterwards glued onto polyester frames, providing stable conditions during the measurements (Fig. 6A). To ensure capturing of diffractograms of transversely and longitudinally oriented fibre bundles within fruit extensions separately, the samples were scanned with an x-ray beam (30 µm diameter) along a line with a step size of 30 µm and an exposure time of 60 s for a single diffraction pattern. The two-dimensional diffraction patterns were collected using an area detector (MarMosaic 225, Mar USA, Evanston, pixel size of 73.2 x 73.2 $µm^2$, distance of 249.5 mm to the sample) and corrected by subtracting a background image (empty beam and dark current measurements). The corrected 2D patterns were radially, then azimuthally integrated over the scattering angle 2Θ of 11°-12.4° (200 Bragg reflection of the crystalline cellulose Iβ) and the microfibril angle determined on the obtained 1D azimuthal curve, assuming circular cell geometry [21-23].

2.6. Scanning electron microscopy (SEM)

To characterise fracture surfaces, air-dried samples were sputter-coated with a 10 nm layer of gold palladium and examined with the SEM Supra 40VP (Carl Zeiss MicroImaging GmbH, Oberkochen, Germany) at an acceleration voltage of 5 kV.

2.7. Data analyses

One-way ANOVA followed by all pair-wise multiple comparison procedure was applied (SigmaPlot 12®, Systat Software, Inc., Richmond, USA), considering the calculated average of double determinations for each sample. Computations of theoretical stress distribution were done using Mathcad 11 (Parametric Technology Corporation).

3. Results

3.1. Theoretical considerations for curved beams

In order to provide a better understanding of the specific microstructure and biomechanics of fruit extensions of Martyniaceae, principal qualitative stress distribution plots in curved beams were visualised in Fig. 2. Commonly, calculated stresses based on the formula in Eq. (2) in accordance with the beam theory including their boundary conditions (straight beams, symmetrical load, pure bending) provided reasonable results, as the radius of curvature R is more than five times the height h of curved beams [24,25]. The ratio R/h differed from 4 to 14 caused by varying cross-sections along the fruit extensions and different curvatures. In curved beams made of an anisotropic and heterogeneous material, characterised by lower strengths in transverse than in the longitudinal axis (fibre reinforced composites, wood), acting radial and/or shear stresses may crucially contribute to failure [25-27]. Such structures and field problems are more accurately described using a two-dimensional plane stress approach in cylindrical polar coordinates r, ϑ, z, where the stress components τ_{rz}, $\tau_{\vartheta z}$, and σ_z are zero (Fig. 2C) [25,28]. During the transport of capsules according to the assumed attachment mechanism and loading by the animal's body weight (F_g), the fruit extensions are dynamically bent by an applied force $F(t)$ de- and increasing the curvature (Fig. 2A). This type of load roughly corresponds to a curved beam clamped at one end carrying a vertical dynamic force at the free end. For simplification allowing an analytical solution, the system was considered as curved beam with an assumed rectangular cross section subjected to a static load (Fig. 2C). The appropriate stress function $\Phi(r,\vartheta)$ is described by the following components

$$\sigma_r = \frac{1}{r}\frac{\partial \phi}{\partial r} + \frac{1}{r^2}\,,\ \sigma_\vartheta = \frac{\partial^2 \phi}{\partial \vartheta}\,,\ \tau_{r\vartheta} = -\frac{\partial \phi}{\partial r}\left(\frac{1}{r}\frac{\partial \phi}{\partial \theta}\right), \quad (5)$$

where σ_r defines the radial stress, σ_ϑ the circumferential and $\tau_{r\vartheta}$ the shear stress. Calculations using the exact solution of Eq. (5) according to Göldner [29], representative geometrical data of fruit extensions (thickness d = 2 mm, α = 45°, R_i (ϑ = 0/30/60°) = 36.0 mm, R (ϑ = 0/30/60°) = 38.0/38.5/39.5 mm, R_o (ϑ = 0/30/60°) = 40.0/41.0/43.0 mm), and an assumed tip

load of 10 N resulted in qualitative stress distribution plots across the beam section, as shown in Fig. 2D. Radial stresses reached up to 4 % of the maximal acting circumferential stresses. Unlike straight beams, the centrally located function maxima for radial stresses shifted up to 7 % towards the concave side of the curvature. Circumferential stresses described a hyperbolic graph, instead of a linear function. Positive tensile stresses result at the inner concave side. The stress maximum of σ_9 at the outer surface was also displaced towards the concave side being a factor of 1.3 higher compared to those of the convex side. Starting from ratios $R/h < 5$, the effect of the hyperbolic stress function profile and increased stresses at the inside of the curved beam were strongly enhanced.

3.2. Mechanical properties of fruit extensions

The Young's modulus of the tested segments of fruit extensions in tensile tests ranged from 6 (2.2) GPa (median (interquartile range)) in *I. lutea* to 9.1 (2.5) GPa in *P. louisianica* (Fig. 3A). Comparative values of pinewood with a rectangular cross-sectional area of 4.6 mm^2 were significantly higher by a factor of 1.4–2.1 (for test statistics see Fig. 3). In that case, the mechanical parameter describes the stiffness of a heterogeneous and anisotropic structure, called structural modulus, which can differ between different load modes [18]. Samples of *I. lutea* failed after loading with 562 (193) N; those of *P. louisianica* and pinewood applying forces of 324 (153) N and 397 (114) N, respectively. Accordingly, this resulted in tensile strength up to twice as high in samples of *I. lutea* (129 (30) MPa) as compared with those of *P. louisianica* (78 (27) MPa) and pinewood (79 (28) MPa) (Fig. 3B). Most fruit extensions initially failed by lengthwise fracturing and afterwards perpendicular combining splintering and shear failure modes. The fracture surfaces were characterised by a strong deformation of cell walls, which was more pronounced in fruit extensions than in pinewood (Fig. 4B–D).

Upon bending loads applied to the concave side of samples, the Young's modulus of fruit extensions was by a factor of 1.6–1.7 higher than loads applied to the convex side (Fig. 3A). Young's moduli of fruit extension (3.6 (1.0) – 7.3 (1.5) GPa) were significantly smaller than that of pinewood samples (11 (2.5) GPa) with comparable section modulus of about 2.1 mm^3 (Fig. 3). While the pine wood samples failed at a maximum bending stress of 99 (55) MPa including strong fragmentations (Fig. 4H), the maximum stresses within fruit extensions of both species were up to 2.2 times larger (143 (26) – 220 (55) MPa, considering only broken samples; Figs. 3B, 4E). The fracture surfaces showed longitudinal fibre bundles that failed after considerable deformations of cell walls at the tension side (Fig. 4G). By contrast, the transverse sclerenchyma exhibited reduced frayed areas of fibres (Fig. 4F, arrows). Upon

bending loads applied to the concave side, most fruit extensions did not break because of slipping over the supports. These samples were not considered in Fig. 3B, however, the decrease of stress-strain-curves took place at similar stresses. The differences in strength between both species were not significant (Fig. 3B).

Fruit extensions of both species exhibited a higher resistance against torsional moments resulting in an about 2.2 times larger shear (torsion) modulus as compared with pinewood (Fig. 3A). It should be noted that this mechanical parameter represents the average of both shear moduli G_{yz} and G_{yx} of an anisotropic material such as wood with the longitudinal axis z. Pinewood samples with a comparable geometrical resistance against torque W_t on averaged 3.1 mm^3 failed at low stresses of 24 (4) MPa by a lengthwise rupture resulting in massive frayed areas and shear fractures in the cell walls of tracheids (Fig. 4L). The stress-twist angle curves of fruit extensions showed a significant higher maximum torsional stress of 43 (17) MPa (Fig. 3B). However, the samples exhibited only minor fractures or did not break (Fig. 4J,K).

3.3. Chemical composition of cell walls

Quantitative analyses of the *Klason* lignin revealed a significantly higher lignin content in fruit extension of *I. lutea* (33.5 ± 0.8 %) compared with *P. louisianica* (28.5 ± 3.2 %, t-test, t = -2.9, P = 0.02; Table 1). The related gravimetrically determined cellulose content amounted in significantly higher values in fruit extension of *P. louisianica* (Mann-Whitney rank sum test, T = 10.0, P = 0.016).

The FTIR spectra of fruit extensions exhibited many qualitative similarities to those of pinewood, noticeable by equivalent absorption bands (Fig. 5A). A reliable quantitative evaluation of these spectra is not given, however, basic trends can be seen in combination with quantitative gravimetric analyses. The most obvious differences were marked at the peaks at 3400 cm^{-1} and 2900 cm^{-1}, characterising the hydrogen bonded (O-H) and C-H stretching absorption, respectively [30]. Within the fingerprint region, fruits of *I. lutea* showed different intensities of the carbohydrate band at 1736 cm^{-1} (Fig. 5B, peak I), denoting stretched unconjugated C=O groups in xylans of hemicelluloses [31]. The associated intensities in *P. louisianica* and the peak at 1722 cm^{-1} of pinewood were weaker. Considering the lignin specific bands including wavenumbers of 1595, 1505, 1462, 1427, 1377, 1269, and 1234 cm^{-1}, pinewood and *I. lutea* had a stronger lignin reference band at 1505 cm^{-1} (peak II) based on purely aromatic skeletal vibrations (C=C) in lignin [30]. While pinewood showed absorptions near 1268 and 1230 cm^{-1} (peak III), characterising the guaiacyl type of lignin,

fruits of Martyniaceae strongly absorbed at 1230 cm^{-1} accompanied by an only suppressed band at 1268 cm^{-1}, pointing to a higher content of the syringyl lignin units [31]. The absorption within the complex carbohydrate band at 1026 cm^{-1} (peak IV), caused by C-O stretching, is strong in pinewood samples, but less in fruit samples of *P. louisianica* and *I. lutea*.

3.4 Cell wall microstructure

Representative two dimensional WAXD scattering patterns are represented in Fig. 6B,C. The calculated microfibril angles (MFAs) of the longitudinal fibre bundles of the endocarp (Fig. 6A) are rather constant and in the range of 34° to 55° for *P. louisianica* and 27° and 45° for *I. lutea* with respect to the longitudinal cell axis (Fig. 6D). The median values (34° for *P. louisianica* and 43° for *I. lutea*) differ significantly (Mann-Whitney rank sum test, T = 13141, $P \leq 0.001$). The data analysis of the scattering patterns of transversal sections also revealed large cellulose fibril angles of the transversal oriented fibres similar to the longitudinal fibre bundles (Fig. 6D1). However, only a few scattering patterns could be analysed since the majority of these transversal oriented cells were not oriented parallel to each other (c.f. Fig. 1D) and perpendicular to the measuring line of the WAXD-analyses, leading to difficulties in the precise interpretation of diffractograms.

4. Discussion

The fruit endocarp and especially the hook-shaped extensions of several species of Martyniaceae are formed by an intriguing system of well-ordered fibres [15]. Since it is presumed that trample burrs interlock with hooves of large mammals, it can be expected that an evolutionary optimisation of the anatomical structure happened with respect to this specific mode of epizoochory. In the present study, the complex endocarp microstructure and its mechanical relevance were elucidated based on data about chemical composition, cell wall ultrastructure, mechanical properties of fruit extensions, and theoretical considerations of stress distributions in curved beams.

4.1. Mechanical properties of fruit extensions

In view of the completely fibrous microstructure, the examined fruit extensions are rather compliant and ductile, however, their strength is high. Comparing both Martyniaceae species under tension and bending, samples of *I. lutea* (*Il*) are more flexible than those of *P. louisianica* (*Pl*). The obtained structural Young's moduli from tensile tests (*Il*: E_t ~6 GPa, *Pl*:

E_t ~9.1 GPa) are comparable to those known for balsa (*Ochroma pyramidale*: E_t ~2.6 GPa) and willow wood (*Salix alba*: E_t ~7.2 GPa), but lower than those of wood of most angiosperms and gymnosperms (e.g., Scots pine: E_t ~12 GPa) [32,33]. Based on measured contact separation forces in tensile tests with single hooks of several fruit burrs (0.3–4.7 mm long), Chen et al. [13] calculated theoretical Young's moduli ranging from 2 to 9.5 GPa. These values correspond partly to those represented in this study, however, no detailed information about the anatomical structure of the fruit hooks is given [12]. Under bending loads, the Young's moduli of fruit extensions of Martyniaceae (E_b ~3.6–7.3 GPa) are similar to those determined for the wood of some self-supporting and climbing lianas [34]. It was noticeable that fruit extensions are more flexible upon loading to decrease the curvature, which is the dominant process during the assumed dispersal mode by animals (Figs. 2A, 3A). The stiffness differs about 1.6-fold between loading of the concave and convex fruit side. These differences may be partly caused by inherent methodological reasons (shear stress-components, slipping), but more probably by microstructural specifics as described later. High breaking forces (F_{max} ~562 N) result in tensile strength up to a maximum of 156 MPa in fruit extensions of *I. lutea*, achieving the strength of ash wood (*Fraxinus excelsior*) used as sports equipment timber [32,33]. Interestingly, the flexural strength of fruit extensions ($\sigma_{b\,max}$ ~143–220 MPa) reaches the upper range of the flexural strength reported for wood [33].

Considering stiffness and strength versus shear stresses applied under torsional loading, fruit extensions exhibit higher shear moduli (G ~1.8 GPa) and torsional strengths (τ_{max} ~42 MPa) than many deciduous wood species [32,33]. Resulting ratios between flexural and torsional stiffness EI/GJ of fruit extensions (0.9–2.6) indicate a high resistance against shear stresses. In contrast, for many other plants, such as non-circular, herbaceous plant stems or petioles, ratios of 4.9–7.7 [35] and for cirrate leaves of rattan palms ratios of 8–14 [1] are known, characterising a rather rigid structure with respect to flexural stiffness.

4.2. Chemical composition and microstructure affecting fruit mechanics

Plant stiffness and strength are a result of the hierarchical organisation of cells and tissues. The orientation of cellulose fibrils within polylamellate secondary plant cell walls, the chemical composition, cell geometry, tissue density, as well as the specific arrangement of cells and tissues are crucial factors [e.g., 9,10,18,36-38]. Tensile properties are e.g. influenced by micro- and ultrastructural characteristics [10,35]. Dominant influences are cell orientation, density, and the cellulose microfibril angle (MFA) in (the predominant) secondary cell wall layers. Large microfibril angles result in large strains and low Young's moduli, small MFAs

in small strains and large Young's moduli along the cell axis [10,37,38]. The MFA can vary across the plant stem and also differs across different cell wall layers [39,40]. In secondary cell walls of spruce the cellulose orientation can range from ~5° to angles higher than 45°. Typical values for adult wood, such as the tested *Pinus sylvestris*, are in the range of 10° [41]. The considerable large MFA (27-55°; Fig. 6D,D1) in both the longitudinal and transverse sclerenchyma of fruit extensions results in reduced stiffness of cell walls allowing large strains along at the longitudinal cell axis and a marked flexibility compared to pinewood samples (Fig. 4A,E). According to this relationship, the higher flexibility as a reaction on loads decreasing the curvature of fruit extensions in bending tests may be explained (Fig. 3A). In this case, circumferential tensile stresses act at the outer concave side of fruit extensions, while radial/transverse stresses correspond primarily to tensile stresses [7,8]. The radial stresses reach a maximum at the shifted neutral axis (Fig. 2D) reinforced by transversely oriented fibres, which can easily be stretched due to the large MFA. Loads increasing the curvature of a curved beam induce circumferential tensile stresses at the convex side. Acting radial stresses located inside the beam, however, are primarily of compressive character [8].

Besides the cellulose crystallinity in fibre cell walls, also the MFA contributes to the high strength (Figs. 3B, 4A,E). The tendency of decreased tensile strength at larger MFAs has been shown for pinewood [37]. Differences in tensile strength between *I. lutea* and *P. louisianica* confirm this relationship. The comparatively smaller strength of pinewood may cause by combined effects of microfibril orientation, a more brittle material based on a different chemical composition (high lignin content) and a lower density. Furthermore, a lower sample crystallinity index may play a role, even though differences between pinewood and fruit extensions of Martyniaceae were small (data not shown). Large strains of *I. lutea* during tensile tests may be facilitated by a higher content of xylans (Fig. 5B). Stress-strain curves of wet sclerenchyma strips of *Aristolochia* with extracted amorphous hemicelluloses are characterised by a strong reduction in tensile strain and an early fracture at an extension where in the untreated case the transition point of a biphasic curve is situated [36].

The chemical components of fibre cell walls of fruit extensions resemble those of 'normal' tree wood, evident from similar FTIR spectra of pinewood (Fig. 5). Basic trends can be seen in combination with quantitative gravimetric analyses. Higher intensities of the lignin reference band (peak at 1505 cm^{-1}; Fig. 5B) in samples of scots pine and *I. lutea* point to interspecific differences in Martyniaceae, confirmed by the higher content of *Klason* lignin in *I. lutea* than in *P. louisianica* ($P = 0.02$; Table 1). As expected, the structure of lignin differs between the tested species. In fruit extensions of Martyniaceae, syringyl lignin units (peak at

1230 cm^{-1}) exceed the intensities of the characteristic peak for the guaiacyl lignin type (1268 cm^{-1}), as generally known from angiosperm woods. By contrast, in scots pine as a conifer the absorption at 1268 cm^{-1} dominates [30,31].

The structure of fracture surfaces after mechanical failure implies that the intriguing arrangement of entwined and pervaded parallel fibre bundles in fruit extensions does not play a prominent role in sample stability upon the performed static tensile loading. Besides delamination between fibres of the transverse sclerenchyma (inter-cell failure mode), longitudinal fibre bundles were partially pulled-out from transverse sclerenchyma or ruptured (trans-wall failure mode; Fig. 4B,C). The larger amount of frayed cell walls in fruit fibres compared to pinewood tracheids point to a considerable work of fracture, which is characteristic for ductile materials and enabled by the low initial alignment of cellulose microfibrils to the long axis of fruits (Fig. 6). However, the material behaviour of the curved fruit extensions under bending is distinctly influenced by the structural organisation of fibres. While the 'wrapping-round-effect' is less marked at small strains (elastic range), at higher strain rates, the circular encompassed parallel fibre bundles are stabilized, especially at the compression side of fruit extensions. That type of reinforcement against buckling at the tissue level corresponds roughly to the function of lignin at the cell wall level, which protects cellulose fibrils, e.g., in fibre caps of vascular bundles in slender monocotyledonous plants [42,43]. Furthermore, the splitting up of fibres on the tension side may be delayed, which frequently induces failure (diffuse fracture) of tree branches with a moderate density [7,8]. As curved fruit extensions are straightened, it is likely that early longitudinal cracks among the fibre bundles, provoked by radial (transverse) stresses [7,8,26], are hindered. Particularly, that mechanism plays an important role during the dynamical mammal locomotion, where the fruit extensions continually loaded by tensile and compression forces. SEM images of fracture surfaces confirm that longitudinal fibres mainly remain connected in bundles (Fig. 4F). At the tension side of specimens, we observed both trans-wall failures in transverse sclerenchyma fibres (Fig. 4F, arrows), and ruptured fibres in longitudinal bundles. The apparent more ductile mode of failure in bundles points to large deformations of these longitudinally oriented cells (Fig. 4G), confirming the calculated higher circumferential stresses σ_ϑ compared to radial stresses σ_r at bending (Fig. 2D). By contrast, pinewood breaks under a distinctive 'splintering' mode and all radial reinforcing rays are ruptured (Fig. 4H). That failure is attributed to the known reduced radial strength in wood, although the ray parenchyma considerably contributes to radial strength and inhibits the propagation of microcracks [44,45]. Similar trends can be suggested for the performed torsion experiments,

where only minor defects are observable in samples after reaching the maximum stress (Fig. 4J). By means of transversely elongated cells, which encompass longitudinal fibre bundles, sliding and twisting of bundles against one another is made more difficult, causing a higher torsional modulus. It is conceivable that radial forces may be partly shifted towards the transverse sclerenchyma, resulting in a delayed failure of fruit extensions at larger twisting angles. By contrast, transverse forces in pinewood induce inter-cell failure modes between tracheids, which provoke early longitudinal intercellular cracks and splintering shear fractures in cell walls, due to the lower radial strength (Fig. 4L).

Crack resistant plant materials are known especially from nutshells reinforced by clusters of fibres and fibre-like sclereids, which are arranged in various directions ('parquet pattern') [46]. The animal kingdom provides examples for similarly complex organised, tough materials, e.g. nacre shells or the shark tooth enamel [47,48]. The latter is structured by axially oriented flouroapatite crystallite bundles pervaded by numerous radial bundles [47]. An outer layer of circumferential bundles of crystallites distally enclosed these structures. Hierarchically organised and structurally anisotropic fibrous elements are well known to be important features leading to a great fracture resistance in biological materials [46-49]. Damage tolerance mechanisms based on plasticity (intrinsic toughening) and the crack bridging (extrinsic crack-tip-shielding). These processes involve an effective crack deflection and twist, reduced local stresses at the crack tip, and the spanning of micro-cracks hindering crack propagation [48,49]. At the cell wall level, the large micro-fibril angle causes a structural plasticity of fruit extensions of Martyniaceae. At the tissue level, micro-cracks between axial fibre bundles are spanned analogous to a circular anchor.

We assume that the flexibility and ability to cope with forces that straighten and close the curved fruit extensions seem to ensure the interlocking with hooves of large animals during dynamical locomotion without failure. Released seeds may be dispersed over long distances by grazing mammals, proven for multiple seed-containing diaspores [4-6]. The sophisticated tissue microstructure suggests that fruits of *Ibicella* and *Proboscidea* are adapted to withstand high forces, even though the evolutionary pressure on the plants may have decreased because of the influence of livestock and the question about the original mode of dispersal has to remain unanswered here.

5. Conclusions

The present study gives insight into intriguing, functionally adapted epizoochorous fruits of the plant family Martyniaceae, comprising morphological and microstructural adaptations. By

means of a detailed mechanical, microstructural, and compositional characterisation of the curved fruit extensions we demonstrate that (1) the flexibility upon tensile and bending loads, (2) the high strength of fruit extensions, and (3) their 'benign' failure are attributed to both the cell wall composition and specific structural arrangement of tissues. While thick-walled fibres densely packed in bundles along the longitudinal fruit axis and the high cellulose crystallinity in cell walls positively affect the strength, a large microfibril angle coupled with greater strain rates result in an increased flexibility upon tensile and bending loads. Acting radial and shear stresses upon bending are most probably absorbed by transversely oriented fibres, which are exactly arranged at the position of the stress maximum. Transversely oriented sclerenchyma cells, which encompass and pervade longitudinal fibre bundles, shifts the local mechanical properties towards a more transverse isotropic material character and stabilise these bundles against buckling resulting in a more 'benign' failure of fruit extensions during bending and torsion. From the biological viewpoint, the obtained data substantiate previous assumptions about the specific plant dispersal mode. From the engineering perspective, the remarkable organisation of entwined fibre bundles may inspire the development of technical fibre-reinforced composite materials, especially those with curved geometries of narrow radii avoiding cracks or delamination's between single fibres. Computer-controlled weaving combined with tailored fibre placement technologies provide new opportunities for the development of such transferred complex, load conforming fibre arrangements.

Disclosures

There are no conflicts of interest present in this study.

Acknowledgements

This study was funded by the European Union (ERDF) and the Free State of Saxony (C2-13927/2379). The first author thanks also the Graduate Academy of Technische Universität Dresden for financial support and two anonymous reviewers for suggestions that helped to improve the manuscript. Dr. B. Ditsch and B. Höde (Botanical Garden, Technische Universität Dresden, Germany) are acknowledged for the cultivation and provision of plants. Furthermore, we thank Dr. U. Steiner (Dresden University Applied Science, Germany) for XRD measurements, Dr. R. Lehnen (Thünen Institute of Wood Research, Hamburg, Germany) for FTIR spectra, G. Bonk (Institute of wood and paper technology, Technische Universität Dresden, Germany) for wet-chemical analysis, M. Dähne for partial support of

mechanical measurements, as well as Dr. F. Saxe (Max-Planck-Institute of Colloids and Interfaces, Potsdam, Germany) for support in analysing of the microfibril orientation.

References

[1] Isnard S, Rowe NP. The climbing habit in palms: biomechanics of the cirrus and biomechanics of the cirrus and flagellum. Am J Bot 2008;95:1538–47.

[2] Steinbrecher T, Danninger E, Harder D, Speck T, Kraft O, Schwaiger R. Quantifying the attachment strength of climbing plants: A new approach. Acta Biomater 2010;6:1497–504.

[3] Bauer G, Klein M-C, Gorb SN, Speck T, Voigt D, Gallenmüller F. Always on the bright side: the climbing mechanism of *Galium aparine*. Proc R Soc B 2011;278:2233–9.

[4] Pijl Lvd. Principles of dispersal in higher plants. 3rd ed. Berlin Springer; 1982.

[5] Sorensen AE. Seed dispersal by adhesion. Annu Rev Ecol Syst 1986;17:443–63.

[6] Mori SA, Brown JL. Epizoochorous dispersal by barbs, hooks, and spines in a lowland moist forest in central French Guiana. Brittonia 1998;50:165–73.

[7] Mattheck C, Kubler H. Wood. The internal optimization of trees. 1st ed. Berlin: Springer; 1995.

[8] Ennos AR, Casteren Av. Transverse stresses and modes of failure in tree branches and other beams. Proc R Soc B 2010;277:1253–8.

[9] Fratzl P, Weinkamer R. Nature's hierarchical materials. Prog Mater Sci 2007;52:1263–334.

[10] Burgert I, Fratzl P. Plants control the properties and actuation of their organs through the orientation of cellulose fibrils in their cell walls. Integr Comp Biol 2009;49:69–79.

[11] Speck T, Burgert I. Plant Stems: Functional Design and Mechanics. Annual Review of Materials Research 2011;41:169–93.

[12] Gorb E, Gorb S. Contact separation force of the fruit burrs in four plant species adapted to dispersal by mechanical interlocking. Plant Physiol Bioch 2002;40:373–81.

[13] Chen Q, Gorb SN, Gorb E, Pugno N. Mechanics of plant fruit hooks. J R Soc Interface 2013;10:20120913.

[14] Ihlenfeldt HD. Martyniaceae. In: Kadereit JW, editor. Flowering plants dicotyledons: The families and genera of vascular plants. Berlin, Germany: Springer; 2004. p. 283–8.

[15] Horbens M, Gao J, Neinhuis C. Cell differentiation and tissue formation in the unique fruits of devil's claws (Martyniaceae). Am J Bot 2014;101:914–24.

[16] Hossler FE. Ultrastructure atlas of human tissues. Hoboken, New Jersey: Wiley; 2014.

[17] Becker T, Splitthof K, Siebert T, Kletting P. Error estimations of 3D digital image correlation measurements. Proc SPIE 2006;6341.

[18] Niklas KJ. Plant biomechanics: An engineering approach to plant form and function. 1st ed. Chicago, IL: University of Chicago Press; 1992

[19] Grote K-H, Feldhusen J. Dubbel Taschenbuch für den Maschinenbau. 22th ed. Berlin: Springer 2007

[20] Kürschner K, Hoffer A. Cellulose und Cellulosederivate. Zeitschrift für analytische Chemie 1933;92:145–54.

[21] Cave, I.D., 1966. Theory of X-ray measurement of microfibril angle in wood. Forest Prod J 16, 37–42.

[22] Lichtenegger, H., Reiterer, A., Tschegg, S., Fratzl, P. 1998. Determination of spiral angles of elementary fibrils in the wood cell wall: comparison of small-angle X-ray scattering and wide-angle X-ray diffraction., pp.

140–156, In B. G. Butterfield, (ed.) Microfibril angle in wood, Proc. IAWA/IUFRO Int. Workshop on the significance of microfibril angle to wood quality. University of Canterbury, New Zealand

[23] Sarén, M.-P., Serimaa, R., 2006. Determination of microfibril angle distribution by X-ray diffraction. Wood Sci Technol 40, 445–460.

[24] Armenakas AE. Advanced mechanics of materials and applied elasticity. 1st ed. New York: Taylor & Francis Group; 2006.

[25] Boresi AP, Schmidt RJ, Sidebottom OM. Advanced mechanics of materials. 5th ed. New York: Wiley; 1993.

[26] Cheung CK, Sorensen HC. Effect of axial loads on radial stress in curved beams. Wood Fiber Sci 1982;15:263–75.

[27] Lu TJ, Xia ZC, Hutchinson JW. Delaminations of beams under transverse shear and bending. Mater Sci Eng 1994;188:103–12.

[28] Ameen M. Computational elasticity: Theory of elasticity, finite and boundary element methods. 1st ed. Harrow, U.K.: Alpha Science International; 2005.

[29] Göldner H. Höhere Festigkeitslehre. 2nd ed. Leipzig: Fachbuchverlag; 1984. (p 84–7)

[30] Pandey KK, Pitman AJ. FTIR studies of the changes in wood chemistry following decay by brown-rot and white-rot fungi. Int Biodeter Biodegr 2003;52:151–60.

[31] Faix O. Fourier transform infrared spectroscopy In: Lin SY, Dence CW, editors. Methods in lignin chemistry. Berlin: Springer; 1992. p. 83–109.

[32] Wagenführ R. Holzatlas. 5th ed. Leipzig: Carl Hanser 2000.

[33] Gibson LJ. The hierarchical structure and mechanics of plant materials. J R Soc Interface 2012;9:2749–66.

[34] Menard L, McKey D, Rowe N. Developmental plasticity and biomechanics of treelets and lianas in *Manihot* aff. *quinquepartita* (Euphorbiaceae): a branch-angle climber of French Guiana. Ann Bot 2009;103:1249–59.

[35] Vogel S. Twist-to-Bend Ratio and Cross-Sectional Shapes of Petioles and Stems. J Exp Bot 1992;43:1527–32.

[36] Köhler L, Spatz H-C. Micromechanics of plant tissues beyond the linear-elastic range. Planta 2002;215:33–40.

[37] Cave ID, Hutt L. The longitudinal Young´s modulus of *Pinus radiata*. Wood Sci Technol 1969;3:40–8.

[38] Reiterer A, Lichtenegger H, Tschegg S, Fratzl P. Experimental evidence for a mechanical function of the cellulose microfibril angle in wood cell walls. Phil Mag A 1999;79:2173–84.

[39] Peura M, Müller M, Vainio U, Sare´n M-P, Saranpää P, Serimaa R. X-ray microdiffraction reveals the orientation of cellulose microfibrils and the size of cellulose crystallites in single Norway spruce tracheids. Trees 2008;22:49–61.

[40] Gierlinger N, Luss S, König C, Konnerth J, Eder M, Fratzl P. Cellulose microfibril orientation of *Picea abies* and its variability at the micron-level determined by Raman imaging. J Exp Bot 2010;61:587–95.

[41] Barnett JR, Bonham VA. Cellulose microfibril angle in the cell wall of wood fibres. Biol Rev 2004;79:461–72.

[42] Rüggeberg M, Burgert I, Speck T. Structural and mechanical design of tissue interfaces in the giant reed *Arundo donax*. J R Soc Interface 2009;7:499–506.

[43] Wang X, Ren H, Zhang B, Fei B, Burgert I. Cell wall structure and formation of maturing fibres of moso bamboo (*Phyllostachys pubescens*) increase buckling resistance. J R Soc Interface 2012;9:988–96.

[44] Burgert I, Eckstein D. The tensile strength of isolated wood rays of beech (*Fagus sylvatica* L.) and its significance for the biomechanics of living trees. Trees 2001;15:168–70.

[45] Reiterer A, Burgert I, Sinn G, Tschegg S. The radial reinforcement of the wood structure and its implication on mechanical and fracture mechanical properties-A comparison between two tree species. J Mater Sci 2002;37:935–40.

[46] Schüler P, Speck T, Bührig-Polaczek A, Fleck C. Structure-Function Relationships in *Macadamia integrifolia* Seed Coats – Fundamentals of the Hierarchical Microstructure. PLoS ONE 2014;9:e102913.

[47] Enax J, Janus AM, Raabe D, Epple M, Fabritius H-O. Ultrastructural organization and micromechanical properties of shark tooth enameloid. Acta Biomater 2014;10:3959–68.

[48] Chen Q, Pugno NM. Bio-mimetic mechanisms of natural hierarchical materials: A review. J Mech Behav Biomed Mater 2013;19:3-33.

[49] Ritchie RO. The conflicts between strength and toughness. Nat Mater 2011;10:817–22.

Figure Legends

Fig. 1. Spatial tissue arrangement in fruits of Martyniaceae. (A) Plants of *Ibicella lutea* cultivated outdoors at the Botanical Garden Dresden with capsules, (A1) which are shed after desiccation exposing a woody endocarp upon ripening. (B) Matured capsules endocarp with longitudinally splitting hornlike extensions of *I. lutea* (left) and *Proboscidea louisianica* (right). (C, D) Light microscopy images of representative transverse sections in the middle segment of fruit extensions of *P. louisianica* (s1), and (E) the capsule body (s2) encompassing the loculus that contains the seeds. cb, capsule body; ec, endocarp; ex, fruit extension; ls, fibre bundles of longitudinal sclerenchyma; lo, loculus; mc, mesocarp; s1, s2, sectional planes; ts, fibres of transverse sclerenchyma. Scale bars = 2 cm (A, B), 2 mm (C), 300 µm (D, E).

Fig. 2. Theoretical considerations on the functional morphology and anatomy of Martyniaceae fruits. Schematic illustrations (A) visualizing a probable interlocking mechanism of fruit extensions with hooves and ankles of passing mammals stepping onto capsules, and (B) of the endocarp anatomy. Longitudinally arranged fibre bundles (orange) are embedded in a dense mesh of transversely oriented fibres (grey/black). (C) Geometric model of a tip loaded curved beam including relevant parameters. (D) Qualitative distribution plots of calculated theoretical radial stresses σ_r and circumferential stresses σ_ϑ (positive values denote tensile, negative compressive stresses) across the section (from R_i to R_o) for different distances from the tip load. Dark grey lines mark the concave side of the extension; light grey lines the convex side. *C*, centre of the curvature; *F*, tip loading force; F_g, weight of the animal; M_i, $F_{i\vartheta}$, F_{ir}, internal forces; $R(\vartheta)$, radius of the centroid of cross-section; $R_i(\vartheta)$, inner radius of curvature; $R_o(\vartheta)$, outer radius; $r+\Delta r(\vartheta)$, radius in polar coordinates system; α, angle of tip load; ϑ, angle in polar coordinates system.

Fig. 3. Mechanical properties of fruit extensions of Martyniaceae (*Pl*: *P. louisianica*, *Il*: *I. lutea*) in comparison with those of pinewood samples (*Pi*) of comparable geometrical resistance parameters: (A) the Young's modulus, shear modulus, and (B) strength, determined in tensile, three-point-bending, and torsion tests (indicated by the pictograms at the top, please note the varying scale). The number of samples (n) and the level of significant differences, revealed by subsequently performed pairwise comparisons within the groups (brackets) of each loading mode are included: ***p<0.001; **p<0.01; *p<0.05; n.s., p>0.05 (Test statistics: one way ANOVA followed by all-pairwise multiple comparison procedure Holm-Sidak test, P = 0.01; the modulus in tensile tests: $F_{2,77} = 69.8$, $P \leq 0.001$; the modulus in bending tests: $F_{4,142} = 133.6$, $P \leq 0.001$; the tensile strength: $F_{2,76} = 59.1$, $P \leq 0.001$; the flexural strength: $F_{4,69} = 51.0$, $P \leq 0.001$; for torsion tests: Kruskal-Wallis one-way ANOVA on ranks followed by all-pairwise multiple comparison procedure Dunn's method, P = 0.05; the shear modulus: $H_{2,79} = 50.0$, $P \leq 0.001$; the strength: $H_{2,65} = 41.9$, $P \leq 0.001$).

Fig. 4. Representative stress-strain/deformation-diagrams (A, E, I) and SEM images visualising failure surfaces in pinewood (*P. sylvestris*; D, H, L), and fruit extensions of Martyniaceae (*P. louisianica* and *I. lutea*; all others) after they were loaded (A-D) in tensile, (E-H) three-point-bending, and (I-L) torsion tests. ls, fibre bundles of longitudinal sclerenchyma; tr, wood tracheids; ts, fibres of transverse sclerenchyma; wr, wood rays. Scale bars = 200 µm (B, F, H, J, L), 50 µm (C, D, G, K).

Fig. 5. FTIR spectra of fruit extensions of Martyniaceae (*P. louisianica* and *I. lutea*) compared with pinewood (*P. sylvestris*) samples: (A) at the complete range of measurements, and (B) within the fingerprint region. Characterised absorption bands, which comprised differences among the samples, are highlighted and magnified in Roman numbered boxes.

Fig. 6. WAXD-analyses. (A) Experimental preparation setup with an indicated (1) longitudinal / (2) transversal sectional plane and examined longitudinal section of fruit extensions of *I. lutea*. (B,C) Representative 2D scattering images of (B) *P. louisianica* and (C) *I. lutea*. (D) Calculated microfibril angles across longitudinal and (D1) transversal sections of *P. louisianica* (dark grey) and *I. lutea* (light grey). Different samples are characterised by changed symbols.

Tables

Table 1.

Klason lignin and cellulose content of fruit extensions of Martyniaceae (*P. louisianica* and *I. lutea*) compared with pinewood

Species	*Klason* lignin content (%)		Cellulose content (%)	
	n	(mean ± sd)	n	(mean ± sd)
P. louisianica	5	28.5 ± 3.23	5	56.1 ± 1.90
I. lutea	4	33.5 ± 0.76	4	49.8 ± 2.02
P. sylvestris		26.3...31.4 [1]		41.9...52.2 [1]

[1] data according to [32]

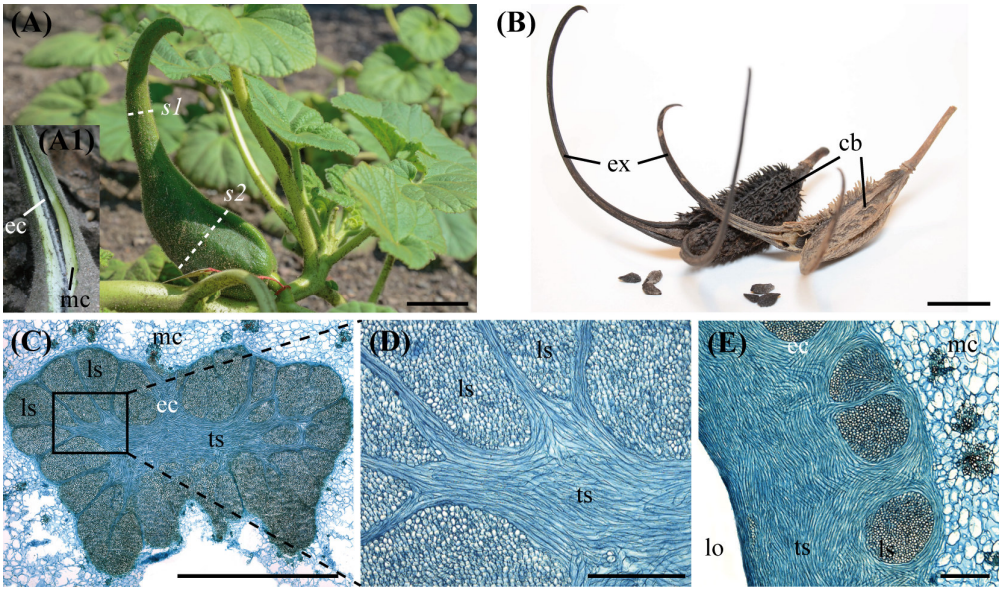

Fig. 1

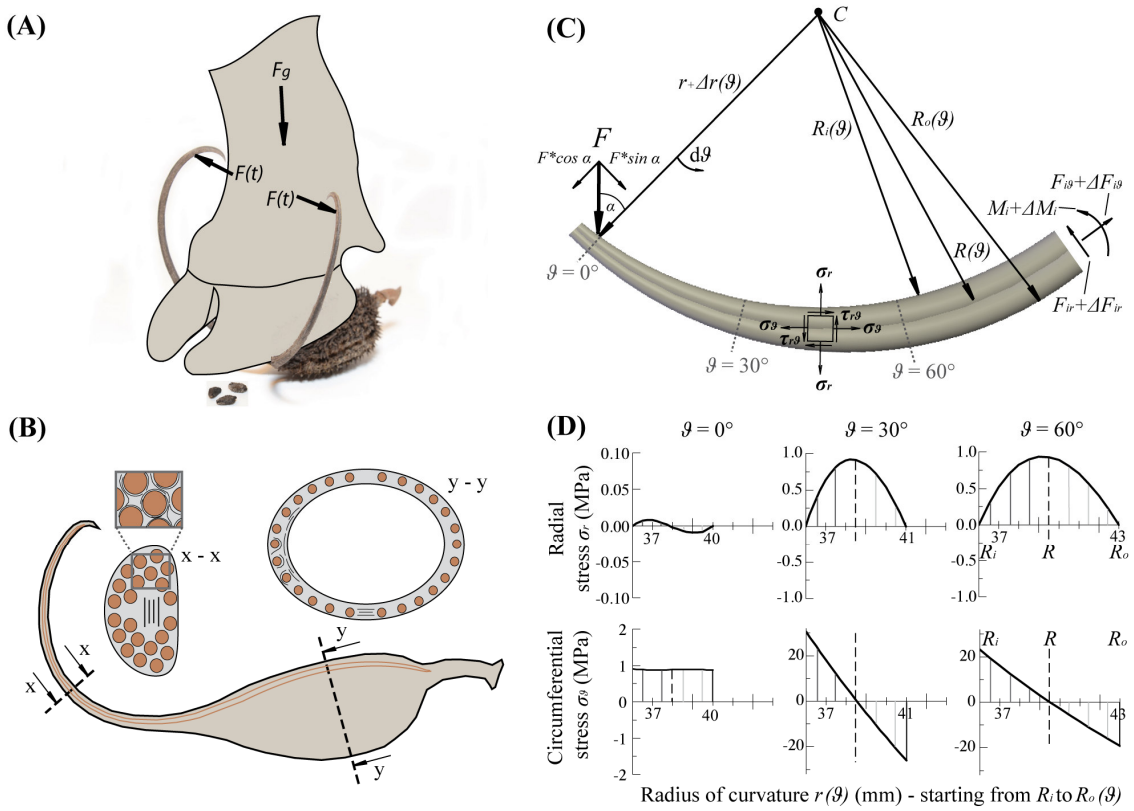

Fig. 2

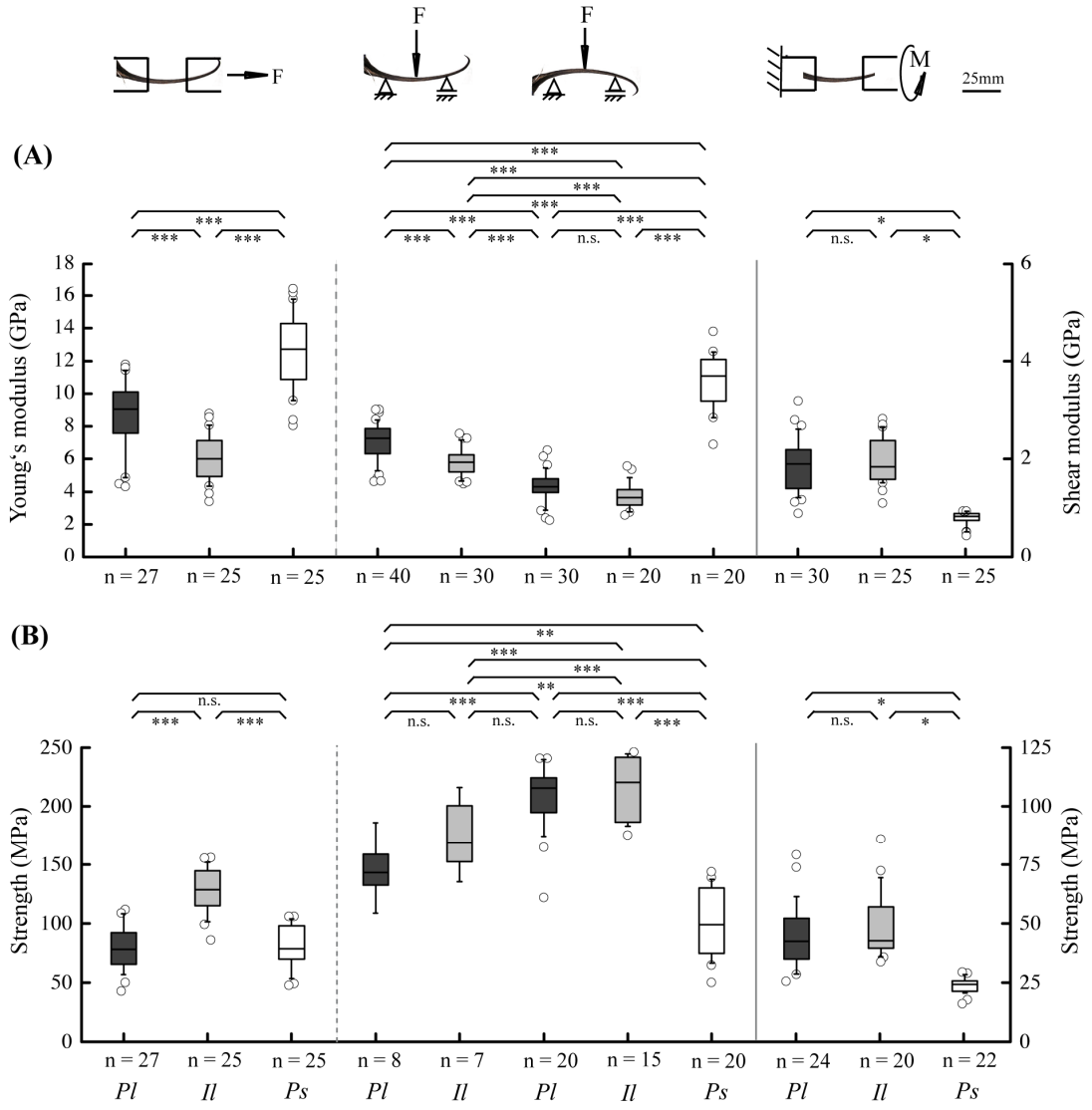

Fig. 3

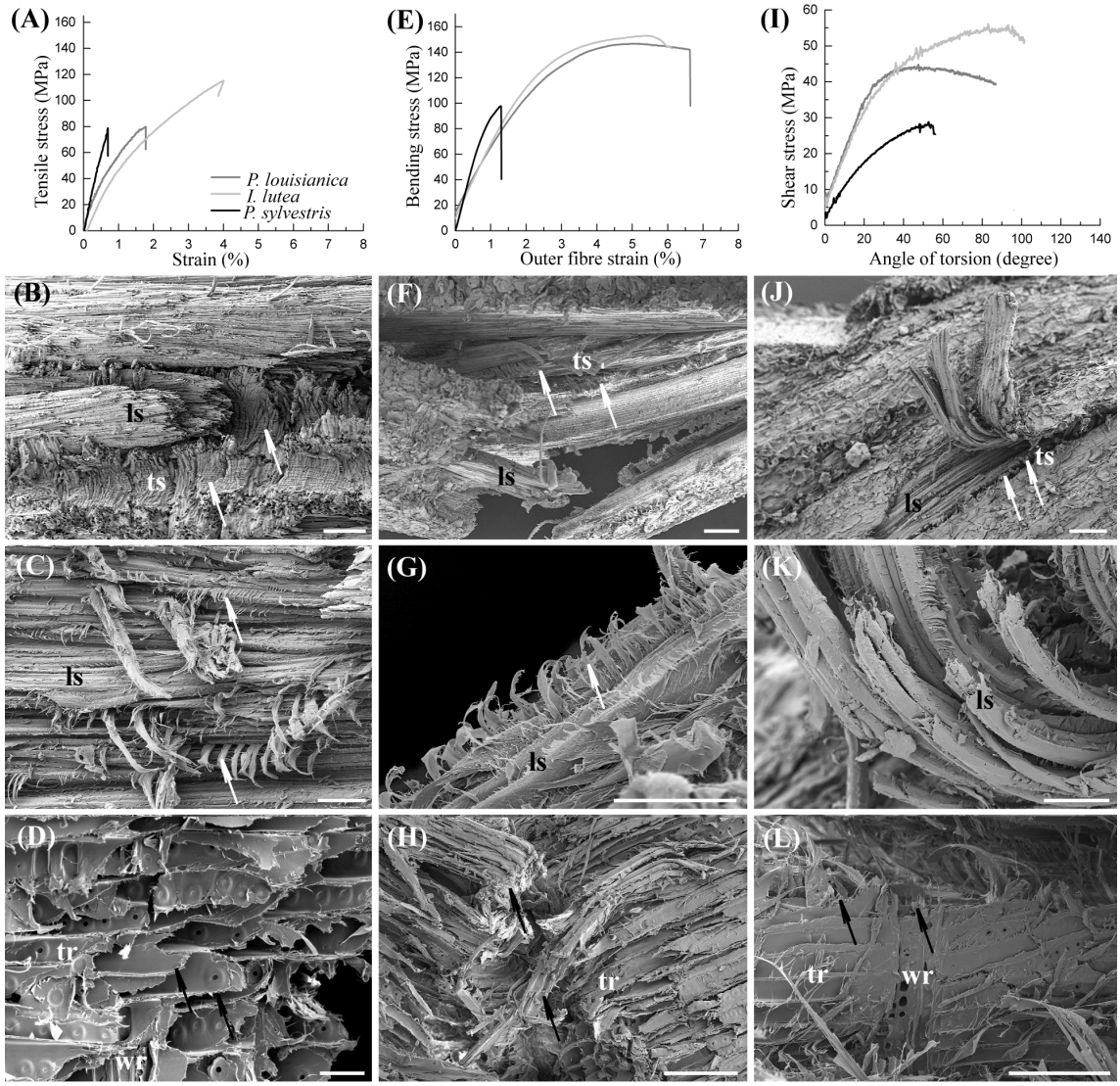

Fig. 4

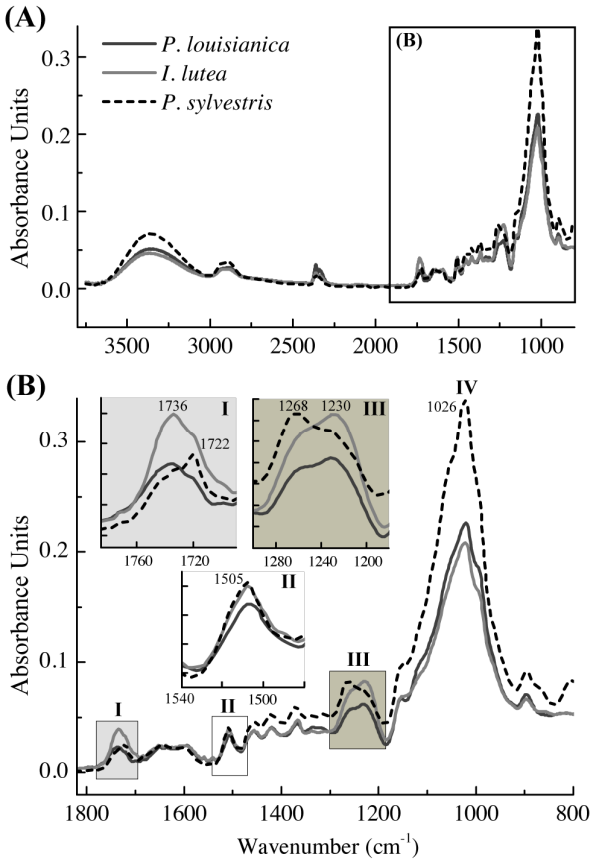

Fig. 5

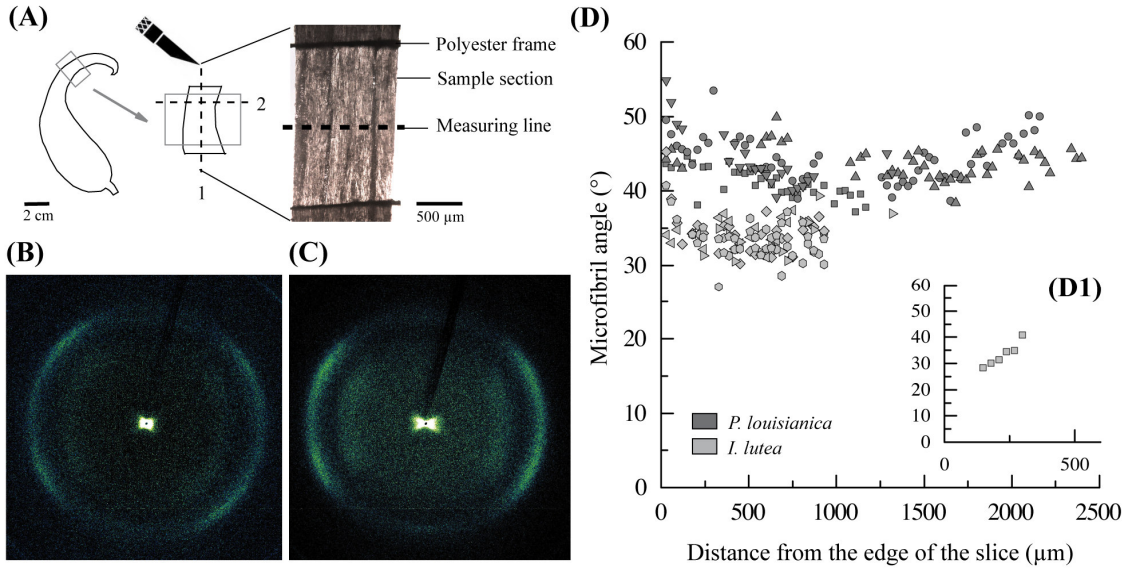

Fig. 6

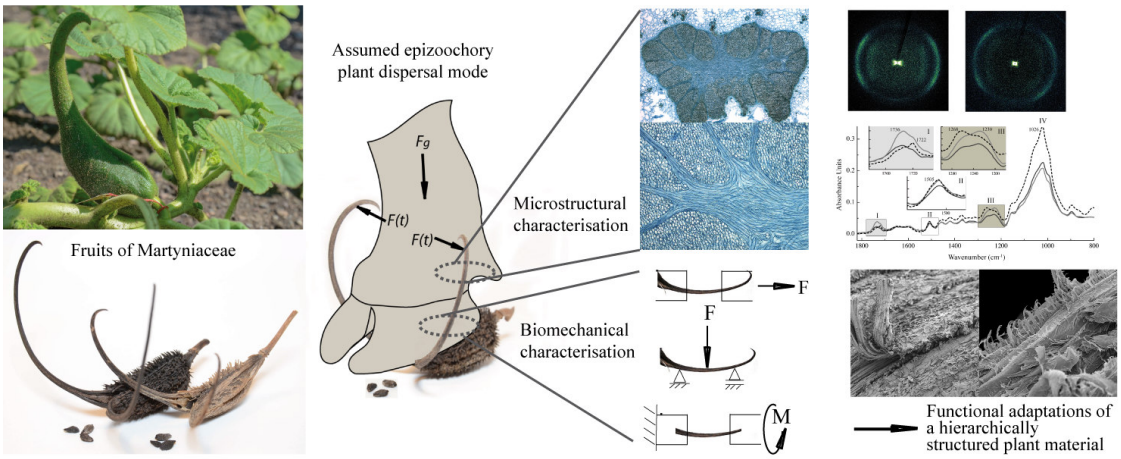

Graphical abstract